molecular pharmaceutics

ARTICLE

pubs.acs.org/molecularpharmaceutics

Intracellular Targeting of PLGA Nanoparticles Encapsulating Antigenic Peptide to the Endoplasmic Reticulum of Dendritic Cells and Its Effect on Antigen Cross-Presentation *in Vitro*

Hadas Sneh-Edri,[†] Diana Likhtenshtein,[†] and David Stepensky*

Department of Pharmacology, Ben-Gurion University of the Negev, Beer-Sheva, Israel

ABSTRACT: Intracellularly targeted delivery system based on PLGA nanoparticles decorated with endoplasmic reticulum (ER)-targeting or control peptides and encapsulating antigenic peptide and fluorescent marker, was developed and characterized. The cellular uptake by dendritic cells (murine DC2.4 cells), intracellular trafficking, and cross-presentation efficiency of this delivery system were studied *in vitro*. The prepared nanoparticles (an average diameter of ~350 nm) efficiently encapsulated antigenic peptide and fluorescent marker and gradually released them over several days. Yet, the nanoparticles' size was small enough to allow their efficient endocytosis by the antigen-presenting cells *in vitro*. Surface conjugation of the targeting or control peptides enhanced the endocytosis of the nanoparticles, affected their intracellular trafficking, and induced prolonged low-magnitude cross-presentation of the antigenic peptide. We demonstrated *in vitro* that the intracellular fate of nanoparticulate drug delivery systems can be altered by their surface decoration with peptidic targeting residues. More detailed investigation is required to determine the mechanisms and therapeutic potential of intracellular targeting of nanodelivery systems *in vivo* for the goal of an anticancer vaccine.

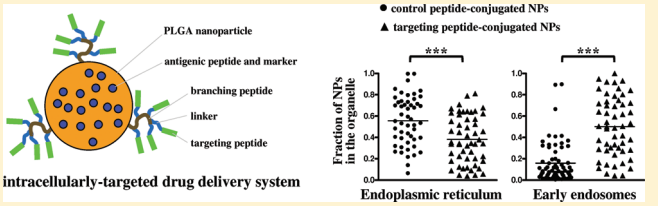

KEYWORDS: targeted drug delivery, intracellular targeting, nanoparticle formulations, antigenic peptide, anticancer vaccination

INTRODUCTION

Many drugs act on intracellular targets and require efficient endocytosis and permeation to the site of action in a specific organelle in order to exert their pharmacological effects. Complexity of the cellular endocytosis and trafficking pathways[1,2] and high compartmentalization of the cells into different organelles lead to suboptimal magnitude and duration of pharmacological effects in the organelle of interest as well as to nonspecific effects due to exposure of other organelles to the drug. Therefore, encapsulation of the intracellularly acting drugs into specialized drug delivery systems (DDSs) that are targeted to specific organelle and deliver the drug in a controlled fashion is required in order to obtain efficient and selective pharmacological effects.[3,4] Intracellularly targeted DDSs can be based on drug-encapsulating particles or vesicles (liposomes) decorated with organelle-specific targeting moieties. Efficient targeting of the drug to the organelle of interest requires recognition of the targeting moieties by the endogenous intracellular trafficking mechanisms.[3,4]

Feasibility of targeted delivery of drugs and model compounds into individual organelles has been assessed in several studies (see review[5]) that claim preferential drug delivery to target organelles. Targeting moieties that were used for this purpose included (1) peptide sequences that are recognized by cytosolic transport systems of the host cell, such as endoplasmic reticulum (ER) signal peptide or ER-retrieval sequence, nuclear localization signal (NLS), mitochondrial localization signal, etc.; (2) peptide or nonpeptide molecules that preferentially interact with the membrane of the target organelle, e.g. mitochondriotropic arginine-rich peptides or positively charged compounds. The above-mentioned studies, however provide limited quantitative and mechanistic insights into effect of organelle-specific targeting residues on the intracellular trafficking of nanoparticle formulations and its effect on the resulting pharmacological activities of the drug.

In this research project we sought to perform quantitative assessment of intracellularly targeted nanoparticulate DDS and to determine the effect of the targeting ligands on the nanoparticles' intracellular localization and the drugs' pharmacological effect. To this end, a delivery system was developed for intracellularly targeted drug delivery (see Figure 1) and its *in vitro* efficiency assessed in experimental cells. An experimental setup was applied based on the delivery of an antigenic peptide to antigen-presenting cells comprising one of the steps of cancer immunotherapy using anticancer vaccines.[6,7] For efficient vaccination, antigenic peptides should reach the intracellular organelles within the antigen-presenting cells where the antigen cross-presentation process takes place (predominantly the ER and endosomal compartments).[8] The setup and the specific antigenic peptide (SIINFEKL) were chosen based on the availability of specific and highly sensitive reagents and experimental systems (specific antibodies and assays) needed for quantitative

Received: February 2, 2011
Accepted: June 10, 2011
Revised: May 31, 2011
Published: June 10, 2011

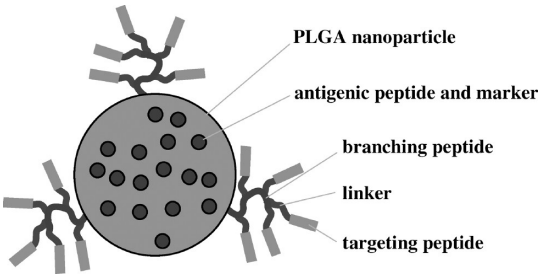

Figure 1. The developed formulation for intracellularly targeted drug delivery. The formulation was based on PLGA nanoparticles loaded with antigenic peptide and fluorescent marker (SIINFEKL and BSA-FITC, respectively). The decoration of the nanoparticle surface was performed by stepwise conjugation of the branching peptide, linker, and targeting or control peptide.

assessment of the intracellular fate and pharmacological effect (i.e., cross-presentation efficiency) upon application of the targeted delivery nanoparticles or control formulations. We choose to assess targeting to the ER since this organelle is a major site of peptide loading on the MHC class I molecules, and efficient delivery of exogenous peptide to this organelle can dramatically enhance its cross-presentation efficiency. As a targeting signal we used a peptide containing specific ER-targeting moieties (KKXX signal) that was previously shown to target intracellular proteins to the ER.[9,10]

MATERIALS AND METHODS

Materials, Antibodies and Cells. Poly(DL-lactide-*co*-glycolide) polymer (PLGA, 50:50 monomer ratio, with free carboxylic end groups, MW 31−58 kDa) was from LACTEL (DURECT Corp., USA). SIINFEKL, branching (ADGADGADG), and propiolic acid N-conjugated targeting (AAKKAA) and control (scrambled, KAAAAK) peptides were synthesized by GL Biochem, China. The peptides were synthesized using a regular Fmoc solid phase synthesis method, and propiolic acid was attached to the amino group of N-terminal residue of the targeting and control peptides at the last elongation step, followed by the regular deprotection, cleavage and ashing steps. Bovine serum albumin labeled with fluorescein isothiocyanate (BSA-FITC), poly(ethylene-*alt*-maleic anhydride) (PEMA), *N*-(3-dimethylaminopropyl)-*N*′-ethylcarbodiimide hydrochloride (EDC), *N*-hydroxysuccinimide (NHS), 2-(*N*-morpholino)ethanesulfonic acid (MES), and chlorophenol red-β-D-galactopyranoside (CPRG) were from Sigma-Aldrich (Rehovot, Israel). DMSO, ethanol, methanol, isopropanol, dichloromethane, and other analytical grade solvents were from BioLab, Israel. All other reagents were of analytical grade.

The following antibodies were used: rat monoclonal antibody against GRP94 (ER marker; clone 9G10, SPA-850, Stressgen), rabbit anti-EEA1 polyclonal antibody (early endosomes marker; 50313, Abcam), mouse monoclonal antibody that recognizes of H-2K^b-SIINFEKL complexes (25-D1.16 clone, generously provided by Prof. Lea Eisenbach, The Weizmann Institute of Science, Israel), Alexa Fluor 594 donkey anti-rat IgG (Invitrogen), Alexa Fluor 546 F(ab')$_2$ fragment of goat anti-rabbit IgG (Invitrogen), and Cy5-conjugated donkey anti-mouse IgG (Millipore).

DC2.4 mouse dendritic cells (H-2K^b-positive, immature cells) and B3Z cells (lacZ-inducible CD8-OVA 1.3 T-T hybridoma cells that recognize SIINFEKL-H-2K^b complexes[11]) were kindly provided by Prof. Peter Cresswell, Yale University, CT, USA. DC2.4 cells were cultured in RPMI 1640 medium (Biological Industries, Beit-Haemek, Israel) supplemented with 10% fetal bovine serum, 2 mM L-glutamine, 50 mg/mL gentamycin sulfate, 1% nonessential amino acids, and 50 μM β-mercaptoethanol. B3Z cells were cultured in the same medium lacking β-mercaptoethanol. Both types of cells were grown in a humidified atmosphere with 5% CO_2 and 37 °C, and undergo incubation with the studied formulations at the same conditions (see below).

Nanoparticle Preparation. Nanoparticles were prepared by a double emulsion technique (w/o/w emulsion). A solution of BSA-FITC and SIINFEKL in PBS (2 mg/mL of each component, 200 μL) or PBS (to generate empty nanoparticles, a negative control) was added to a solution of PLGA in dichloromethane (100 mg/mL, 2 mL), and sonication was performed using Vibracell probe sonicator (Sonics, CT, USA) with probe No. 3 for 2 min on ice. To the resulting w/o emulsion was added an aqueous solution of PEMA (20 mg/mL, saturated with DCM, 5 mL), and sonication was carried out for 5 min at the same conditions to form a w/o/w emulsion. This emulsion was transferred to an aqueous solution of PEMA (3 mg/mL, 50 mL) and vigorously stirred for 5 min. After that, an aqueous solution of PEMA with isopropanol (9:1, v:v, 50 mL) was added and the formulation stirred for 3 h in the chemical safety cabinet for complete evaporation of the organic solvents. The nanoparticles were sedimented by centrifugation, washed, resuspended in double distilled water and lyophilized using FreeZone 2.5 Plus Lyophilizer (Labconco, MO, USA).

Decoration of the Nanoparticles' Surface with Targeting Residues. At the first stage, a branching peptide was conjugated to the nanoparticles' surface using a carbodiimide reaction. The nanoparticles (10 mg) were resuspended in MES buffer (100 mM, pH 5.8) and underwent a reaction with EDC and NHS (10 and 5 M, respectively) for 30 min at room temperature. The nanoparticles with activated carboxylic groups were then washed, resuspended in borate buffer (200 mM, pH 8.5), to undergo a reaction with the branching peptide (600 mM) for 2 h at room temperature, and were then washed with PBS (100 mM, pH 7.4).

In the next stage, linker (3-azidopropylamine, 5 M) was conjugated to the nanoparticles decorated with branching peptide using a carbodiimide reaction under the same synthesis conditions. The linker was synthesized from sodium azide and 3-chloropropylamine according to the procedure described by Jiang et al.[12]

In the last stage, the targeting or control peptide was conjugated to the linker using a Click reaction. The nanoparticles decorated with the branching peptide and linker were resuspended in aqueous solution of copper sulfate and sodium ascorbate (100 mM and 500 mM, respectively), propiolic acid N-conjugated targeting or control peptide (1.5 M) was added, and the suspension was incubated for 3 h at room temperature with constant stirring. The nanoparticles were sedimented by centrifugation, washed, resuspended in double distilled water and lyophilized.

The success of the individual conjugation steps was qualitatively assessed by Fourier transform infrared analysis (FTIR). Nanoparticle samples were placed on ZnSe crystals and analyzed using IR Scope II microscope equipped with EQUINOX 55/S FTIR spectrometer (Bruke, MA, USA). Three spectra (in the wavelength range of 600−4000 cm^{-1}) were collected from representative parts of the samples and averaged.

Characterization of the Nanoparticles. Nanoparticle morphology was studied with scanning electron microscopy (SEM). Samples of the lyophilized formulations were placed on carbon adhesive tape, coated with gold, and imaged using a Quanta 200 scanning electron microscope (Hillsbro, OR, USA) at the Institute of Applied Research (Ben-Gurion University, Beer-Sheva, Israel). Quantitative analysis of the SEM images determined nanoparticle size by using ImageJ software (version 1.40C, NIH, USA[13]). Nanoparticle ζ-potential was measured by Laser Doppler Velocimetry using a ZetaPlus instrument (Brookhaven Instruments Corporation Ltd., NY, USA) and double distilled water as dispersion medium in the range of 10−1000 nm at the National Institute of Biotechnology (Ben-Gurion University, Beer-Sheva, Israel).

The encapsulation efficiency was determined by analysis of the supernatants of nanoparticle suspensions (taken in the last stage of their preparation, after evaporation of the organic solvents) using a QuantiPro BCA assay kit (Sigma). *In vitro* release rate of the encapsulated materials from the nanoparticles was determined by incubating 5 mg samples of the formulations in 500 μL of PBS solution (1 mM, pH 7.4) at 37 °C with constant mixing by magnetic stirrer. Samples were centrifuged at 3 h, 1, 2, 3, 4, and 7 days, supernatant was collected and replaced with fresh PBS solution, and the samples were thoroughly resuspended by vortexing. BSA-FITC release in the supernatant was quantified using an Infinite M200 microplate reader (Tecan, Switzerland, excitation at 492 nm and emission at 520 nm), and the released peptides and protein were quantified using QuantiPro BCA assay kit (Sigma). Solutions with known concentrations of BSA-FITC and SIINFEKL served as controls.

Uptake of the Nanoparticles by DC2.4 Cells *in Vitro* and Analysis of Intracellular Localization. In all *in vitro* experiments, DC2.4 cells were grown on 24-well or 96-well plates (100,000 or 40,000 cells/well, respectively) and incubated with the individual formulations or with an equivalent amount of SIINFEKL solution (2 μg/mL of free or encapsulated SIINFEKL).

For assessment of NP uptake, DC2.4 cells were incubated with the individual formulations for 2 h, extensively washed with PBS, and harvested using trypsin−EDTA solution (Biological Industries, Beit-Haemek, Israel), and the cells' fluorescence in the green channel was analyzed using the Guava EasyCyte mini flow cytometry system (Millipore, USA) and FlowJo software (v. 7.6.1, Tree Star Inc., USA).

For analysis of intracellular nanoparticle localization: DC2.4 cells grown on glass coverslips in 24-well plates were (1) incubated with the individual formulations for 2 h, (2) extensively washed with PBS, and then fixed with 2.5% formaldehyde in PBS, (3) permeabilized with 0.1% Triton X-100 solution, (4) stained with antibody against GRP94 (ER marker) followed by AF594 donkey anti-rat secondary antibody, or with an antibody against EEA1 (early endosomes marker) followed by AF546 goat anti-rabbit secondary antibody, and (5) mounted on slides using Mowiol 4-88 with DABCO antifading agent. Cells stained with secondary antibodies and/or incubated with empty nanoparticles were used as controls.

Representative images of the prepared slides at the individual fluorescence channels were sequentially collected with an Olympus FV100-IX81 confocal microscope (Tokyo, Japan) equipped with 60× oil objective. All experimental samples were imaged on the same day using a constant set of imaging parameters (that were initially adjusted to keep all the samples' fluorescence within a linear range). The collected images were analyzed using a custom-written "IntraCell" plugin in ImageJ software[14,15] to identify the borders of the individual cells and the organelles (endoplasmic reticulum and early endosomes), and to quantify the relative amount of the nanoparticles inside and outside these organelles within a specific cell. For each formulation, at least 50 cells were analyzed using this approach.

Analysis of Cross-Presentation. For FACS analysis of cross-presentation, DC2.4 cells were grown on 24-well plates and were incubated for 2 h with the individual formulations or with equivalent amount of SIINFEKL and BSA-FITC solution (2 μg/mL of free or encapsulated SIINFEKL). They were then extensively washed with PBS, harvested using trypsin−EDTA solution, washed, blocked, resuspended in 1% BSA and 0.1% sodium azide solution, and stained with 25-D1.16 antibody followed by Cy5-conjugated donkey anti-mouse secondary antibody. Fluorescence of the cells was analyzed using FACScanto II flow cytometer (BD, USA) and FlowJo software (v. 7.6.1, Tree Star Inc., USA).

For B3Z T cell activation assay of cross-presentation, DC2.4 cells were grown on 96-well plates and were incubated for 2, 4, 24, or 48 h with the individual formulations or with solution of SIINFEKL peptide and BSA-FITC. The DC2.4 cells were then extensively washed with PBS and incubated with B3Z cells for 20 h, the medium was discarded, the cells were lysed with solution containing 0.3 mM CPRG reagent and incubated for 1 h, and absorbance at 630 nm, which is indicative of amount β-galactosidase secreted by B3Z cells, was determined using Infinite M200 microplate reader (Tecan, Switzerland).

Statistical Analysis. The data are presented as mean ± standard deviation. Differences in the studied parameters between the experimental groups were analyzed using two-tailed *t* test or ANOVA with Tukey−Kramer or Dunnett post-test using InStat 3.0 software (GraphPad Software Inc.). The *p* value less than 0.05 was termed significant.

RESULTS

Nanoparticle Preparation and Characterization. Spherical nanoparticles with narrow size distribution were prepared (Figures 2A and 2B). The diameter of unconjugated nanoparticles was 344 ± 75 nm, and the ζ-potential was −32 ± 1 mV, which is consistent with presence of free carboxylic groups on the nanoparticles' surface. Following individual conjugation steps, characteristic changes of the FTIR spectra of the nanoparticles were observed (e.g., appearance of azide peak at ∼2100 cm^{-1} following conjugation of the linker, appearance of triazole ring at 1500−1600 cm^{-1} following conjugation of the targeting or control peptide that indicates successful Click reaction between azide group of the linker and alkyne group of the propiolic-acid N-conjugated peptide), and were consistent with successful conjugation of branching peptide, linker, and the targeting or control peptides. Multistep conjugation procedure did not affect the morphology or the size distribution of the nanoparticles (data not shown), but decreased the ζ-potential to −27 ± 1 mV, consistent with attachment of positively charged targeting or control peptides to the nanoparticles' surface.

The generated nanoparticles efficiently encapsulated the antigenic peptide and marker molecules: the encapsulation efficiency of unconjugated nanoparticles was 33 ± 8%, corresponding to approximately 0.67 mg of SIINFEKL and 0.67 mg of BSA-FITC per each mg nanoparticle weight (i.e., approximately 10^5 and 10^3 SIINFEKL and BSA-FITC molecules per nanoparticle, respectively). Analysis of fluorescence of the samples obtained in

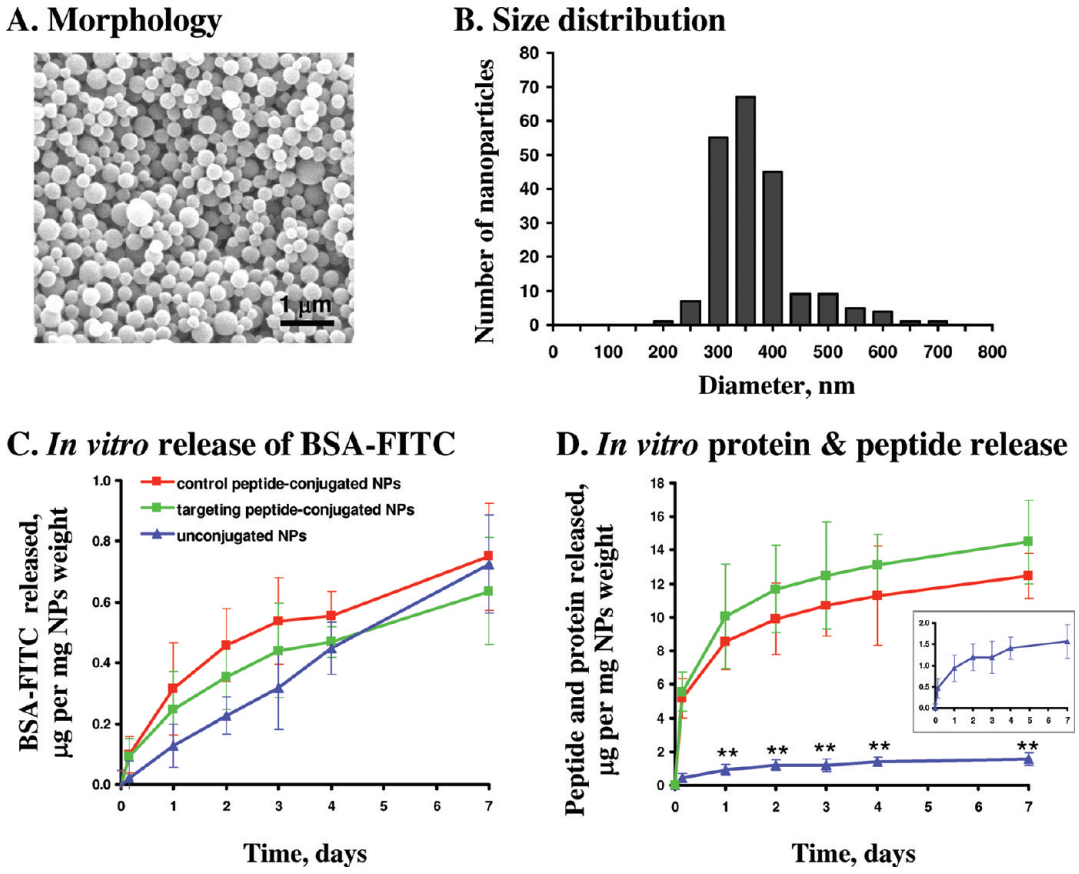

Figure 2. Characterization of the generated nanoparticle formulations. (A) Cryo-TEM analysis of morphology of unconjugated nanoparticles. (B) Nanoparticle size distribution based quantitative analysis of Cryo-TEM images of unconjugated nanoparticles using ImageJ program. Other studied formulations were characterized by similar morphology and size distribution. (C) *In vitro* release of BSA-FITC from the studied formulations into the PBS solution at 37 °C as determined by fluorescence analysis of the samples. (D) *In vitro* release of protein and peptides from the studied formulations into the PBS solution at 37 °C as determined by analysis of the samples using QuantiPro BCA assay. The inset shows a magnified release curve of the unconjugated nanoparticles. The *in vitro* release data curves were obtained following subtraction of background values obtained from samples of empty nanoparticles. Panels A−D present representative data from at least 3 experimental sets for each analysis. The error bars represent SD of triplicates. (**) $p < 0.01$ in comparison to the control and targeting peptide-conjugated nanoparticles (ANOVA with Tukey−Kramer post-test).

in vitro release experiments (see Figure 2C) indicates that BSA-FITC was gradually released from the studied formulations and that the conjugation procedure slightly enhanced its release rate during the first days of the experiment. In addition to BSA-FITC, these samples contained substantial amounts of peptides as can be seen from comparison between content of total protein and peptides vs BSA-FITC alone (see Figure 2D and Figure 2C, respectively). Comparison of these curves for unconjugated nanoparticles indicates that release of SIINFEKL peptide (the only peptide component of this formulation) exhibits a moderate "burst effect" (a phenomenon of rapid release of the surface-adsorbed or superficially located material in the formulation) during the first hours of incubation, followed by gradual release over 3−5 days. On the other hand, targeting and control peptide-conjugated nanoparticles released also substantial amounts of materials that were attached to them during the multistage conjugation procedure (i.e., branching peptide, linker, and targeting or control peptide). We noticed that empty nanoparticles and unconjugated nanoparticles, but not the targeting or control peptide-conjugated nanoparticles, had substantial tendency to aggregate during *in vitro* release experiments. This phenomenon was not observed in other experiments, and none of the studied formulations exhibited tendency for aggregation in the cell medium during cellular uptake and intracellular trafficking experiments, as determined by confocal microscopy of nanoparticles alone, or for cells incubated with the nanoparticles (see below).

Nanoparticle Uptake and Intracellular Trafficking. The endocytosis and intracellular fate of the nanoparticles in the DC2.4 cells was influenced by the presence and sequence of the conjugated peptides. FACS analysis of cells incubated with different formulations indicated significantly higher uptake of targeting or control peptide-conjugated nanoparticles, as compared to the unconjugated nanoparticles (see Figure 3).

Immunofluorescence analysis of both ER and endosomes in the same samples of DC2.4 cells was unsuccessful due to the technical limitations related to the background staining and cross-emission of the fluorophores ("bleed-through" phenomenon). Therefore, staining of the ER and of the endosomes was performed separately (see Figure 4A). Confocal imaging collaborates the conclusions of FACS analysis and indicates that DC2.4 cells were able to endocytose the multiple targeting or control peptide-conjugated nanoparticles, but a significantly smaller number of unconjugated nanoparticles were endocytosed.

Quantitative analysis of the confocal images using custom-written "IntraCell" ImageJ plugin[15] revealed a high colocalization of the nanoparticles with the ER and endosomes, high intercell

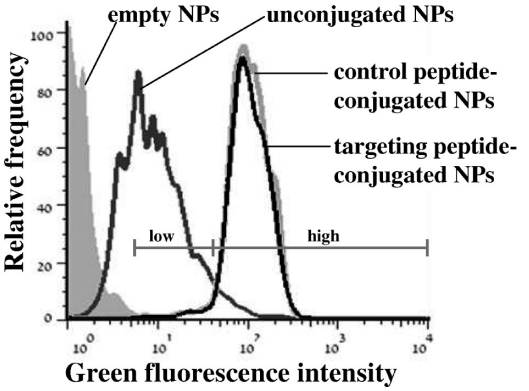

Formulation	low fluorescence	high fluorescence
empty NP	0%	0%
unconjugated NPs	58%	6%
control peptide-conjugated NPs	3%	96%
targeting peptide-conjugated NPs	3%	97%

Figure 3. Uptake of nanoparticle formulations by DC2.4 cells. The cells were incubated for 2 h with the studied formulations in tissue culture incubator at 37 °C, were extensively washed, and were analyzed using FACS to determine efficiency of nanoparticle uptake by individual cells. The table presents relative abundance of cells that endocytosed low or high amounts of the studied formulations. Representative data from 3 experimental sets.

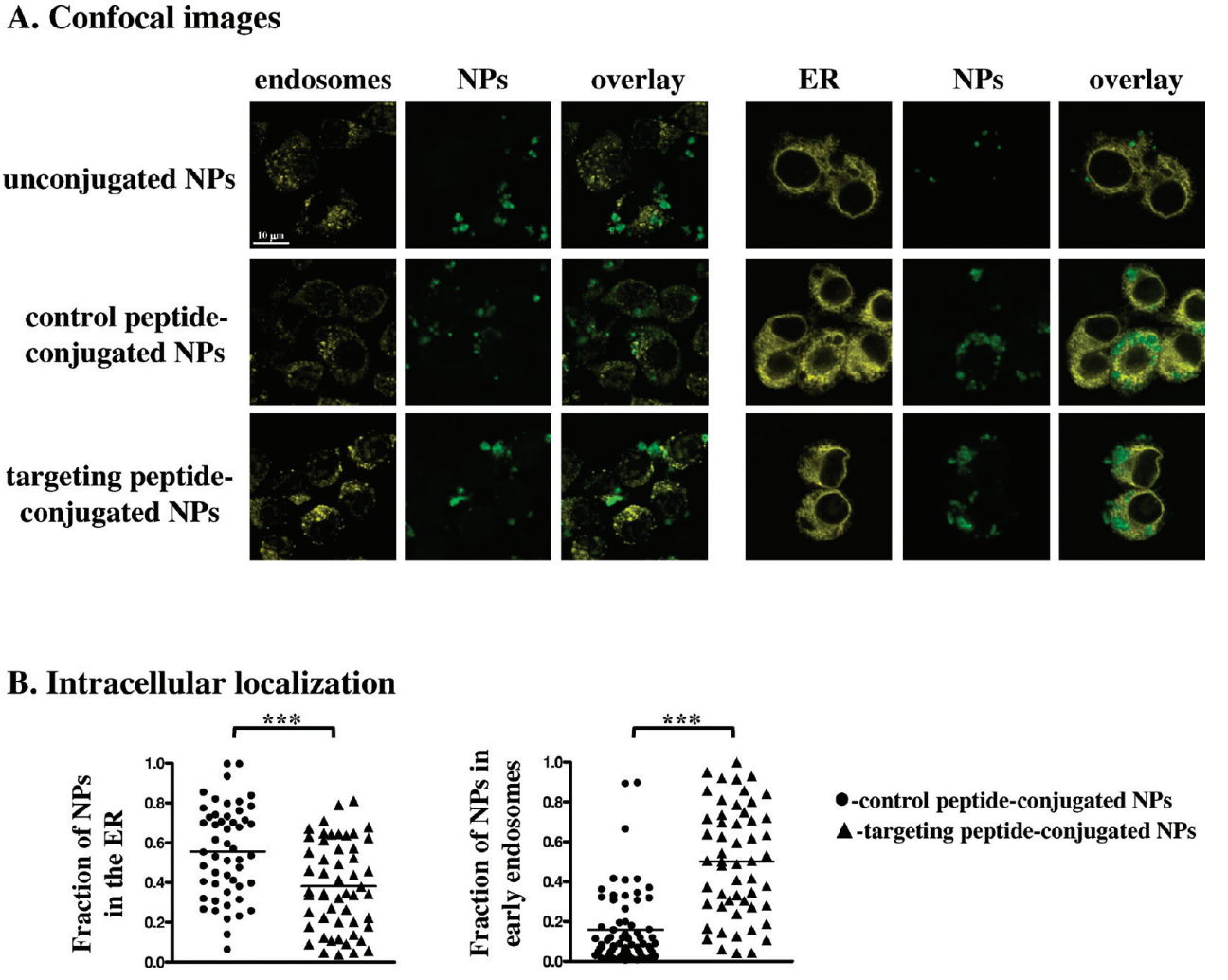

Figure 4. Intracellular localization of nanoparticle formulations in DC2.4 cells. The cells were incubated for 2 h with the studied formulations in tissue culture incubator at 37 °C, extensively washed, fixed with formaldehyde, stained with antibodies against proteins residing in the early endosomes or ER, and mounted on slides. (A) Confocal images of cells incubated with the studied formulations. (B) Relative amount of the control and targeting peptide-conjugated nanoparticles inside the endoplasmic reticulum (ER) and endosomes in the individual cells as determined by custom-written ImageJ plugin. (***) $p < 0.001$ (two-tailed t test).

variability in nanoparticle distribution to these organelles, and significant differences in the intracellular trafficking patterns of the different nanoparticle formulations. Unexpectedly, control peptide-conjugated nanoparticles showed significantly higher

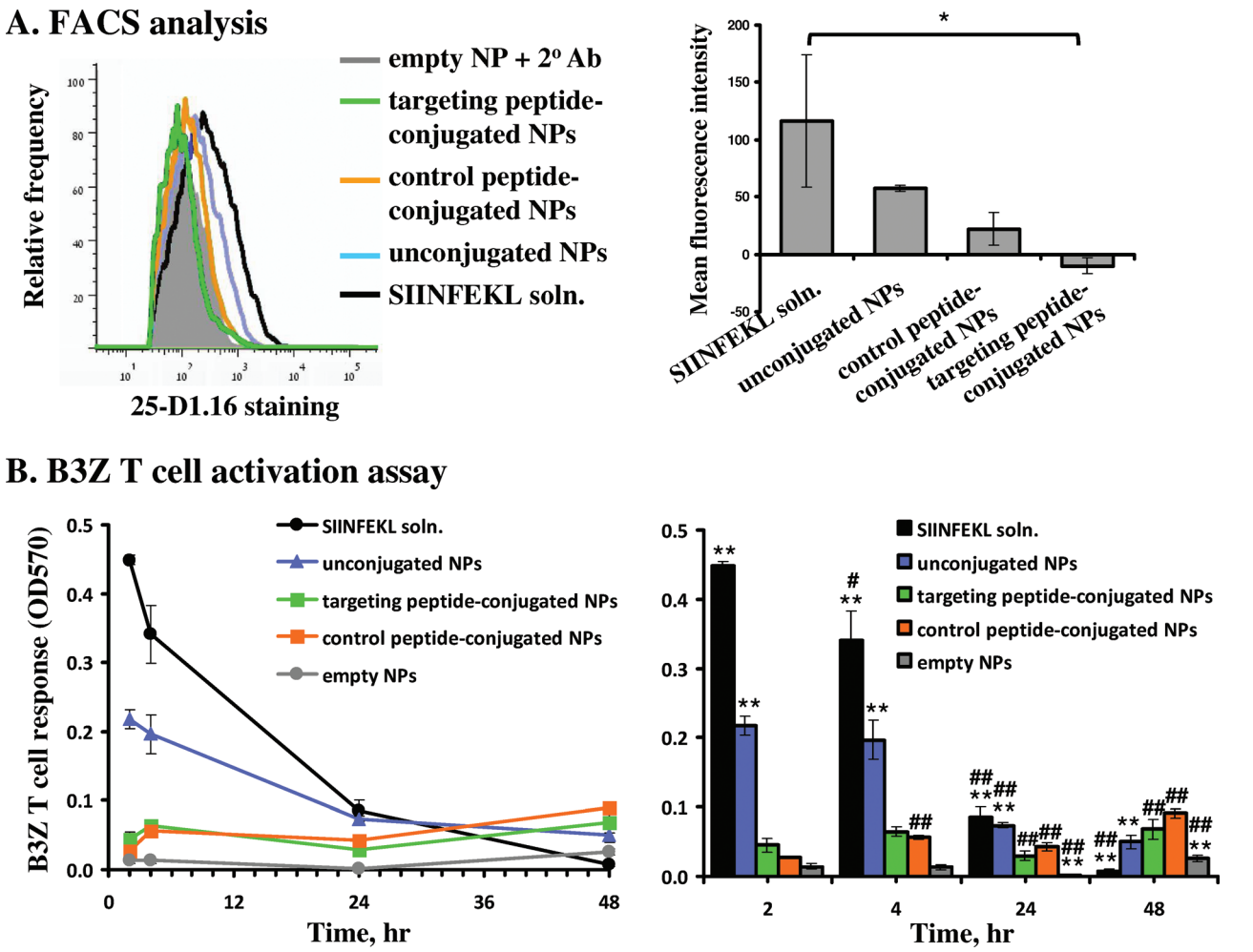

Figure 5. Cross-presentation of the SIINFEKL peptide following incubation of the studied formulations with DC2.4 cells. The cells were incubated for 2 h with the nanoparticle formulations or with SIINFEKL solution (the positive control) in tissue culture incubator at 37 °C, and were extensively washed. (A) Extent of SIINFEKL peptide cross-presentation was quantified by FACS using specific 25-D1.16 antibody. (B) Extent of SIINFEKL peptide cross-presentation was quantified by B3Z T cell activation assay and analysis of β-galactosidase activity of the cells using CPRG reagent. Representative data from 3 experimental sets. The error bars represent SD ($n = 2$ for A, and $n = 3$ for B). (**) $p < 0.01$ in comparison to the control peptide-conjugated nanoparticles (ANOVA with Dunnett post-test). (#) $p < 0.05$, (##) $p < 0.01$ in comparison to the previous time point for the same formulation (two-tailed t test).

accumulation in the ER (0.56 ± 0.23) and a significantly lower accumulation in the endosomes (0.16 ± 0.18), as compared to the targeting peptide-conjugated nanoparticles (0.38 ± 0.22 and 0.50 ± 0.28, respectively, see Figure 4B).

Cross-Presentation Efficiency of the Studied Formulations. Despite high uptake by the cells, control and targeting peptide-conjugated nanoparticles induced low efficiency of SIINFEKL cross-presentation following short-term (2 h) incubation with DC2.4 cells (see Figure 5A and the first time-point of Figure 5B). Unconjugated nanoparticles, however, induced to a higher extent cross-presentation that was comparable to that of the positive control (SIINFEKL solution) and was consistent with a rapid initial release of the peptide from this formulation due to the "burst effect" and efficient cross-presentation of the soluble SIINFEKL peptide.

During longer incubation with DC2.4 cells, control and targeting peptide-conjugated nanoparticles induced prolonged low-magnitude cross-presentation of SIINFEKL peptide (see Figure 5B). Cross-presentation of soluble SIINFEKL was initially high and rapidly declined, whereas unconjugated nanoparticles induced moderate cross-presentation that gradually declined, apparently reflecting a "burst effect" during the first hours of incubation followed by gradual release of SIINFEKL from this formulation. Empty nanoparticles lacking antigenic peptide induced a low but measurable extent of B3Z cell activation (see Figure 5B). This outcome apparently stems from immunomodulatory properties of PLGA nanoparticles that can act as an adjuvant in certain experimental conditions.[16]

DISCUSSION

The Effect of the Targeting Residues on the Uptake and Intracellular Fate of the Nanoparticles. This study investigated intracellular targeting of formulations comprising PLGA nanoparticles decorated with peptidic targeting residues. The formulation was based on several considerations/requirements. For example, the size (diameter) of the particles in the ~200−500 nm range was chosen since such nanoparticles are big enough to

contain a sufficient amount of encapsulated drug (water-soluble antigenic peptide) and gradually release it over several days, yet they are small enough to be endocytosed by the antigen-presenting cells,[17,18] and can be potentially moved intracellularly by the endogenous trafficking mechanisms.[5,19,20] The choice of the polymer (PLGA) was based on presence of carboxylic groups in its chemical structure that are suitable for conjugation of the targeting residues (using a well-studied carbodiimide chemistry in aqueous buffer) that were claimed to enhance nanoparticles' cytosolic delivery following endocytosis ("endosomal escape"[21]). The work was successful in generating nanoparticle formulations with desired properties that were efficiently loaded with SIINFEKL peptide and BSA-FITC marker. *In vitro* release kinetics of the encapsulated material from the unconjugated nanoparticles using two analytical methods (see Figures 2C and 2D) revealed that the encapsulated compounds are gradually released from the formulation. It can be assumed that the difference between curves in panels C and D of Figure 2 originates from release of peptide(s), demonstrating that release of SIINFEKL peptide exhibits a moderate "burst effect" (~30% of the content) during the first hours of incubation, and is slightly more rapid than that of BSA-FITC (3−4 days vs 7 or more days, respectively).

A 3-step conjugation approach was used for stepwise decoration of the unconjugated nanoparticles with the branching peptide, linker, and the targeting or control peptide. To enhance the conjugation efficiency of the targeting residues, we used PEMA as a surfactant/stabilizer (that contains free carboxylic groups[22,23]) and conjugation of branching peptide to increase the number of carboxylic groups on the nanoparticles' surface. The applied conjugations affected the key properties of the formulation, including ζ-potential, FTIR spectrum, uptake and intracellular trafficking in the cells. Outcomes of *in vitro* release experiments indicate that the conjugation procedure had limited effect on the content and release kinetics of BSA-FITC from the nanoparticles. However, effect of the conjugation procedure on the content and release kinetics of SIINFEKL peptide cannot be readily determined as it was masked by release of other peptides from the targeting and control peptide-conjugated nanoparticles. Based on indirect data (kinetics of SIINFEKL release from unconjugated nanoparticles and the overall duration of the conjugation procedure), targeting and control peptide-conjugated nanoparticles are estimated to contain approximately 30% less SIINFEKL in comparison to unconjugated nanoparticles due to its partial release into the aqueous solution (the "burst effect") during the multistep conjugation procedure. On the other hand, targeting and control peptide-conjugated nanoparticles were decorated with high amounts of branching peptide, linker, and targeting or control peptide that were gradually released from these formulations during *in vitro* release experiments (see Figure 2D). Unfortunately, the efficiency of the individual conjugation steps could not be determined due to limited sensitivity and specificity of the available analytical methods. It is expected that the unconjugated PLGA nanoparticles used in this study contained at least several hundred surface carboxylic groups. This estimation is based on report of conjugation efficiency of 433 peptide residues per nanoparticle in a similar experimental system (PLGA nanoparticles of similar size but prepared using polyvinyl alcohol and not PEMA as a surfactant/stabilizer) by Misra et al.[20] PEMA substantially increases the amount of surface carboxylic groups[22,24] and can increase the conjugation efficiency up to thousands of peptide residues per nanoparticle.[25] Based on these reports and the present results of the *in vitro* release experiments, we conservatively estimate that the applied conjugation approach resulted in decoration of nanoparticle surface by at least dozens or hundreds of targeting or control residues.

Intracellular distribution of nanoparticles was characterized by high intercell variability (see Figure 4B) that ranged from 0% to 80−100%. This outcome apparently derives from existence of several competing pathways of nanoparticle endocytosis and intracellular trafficking. It is expected that the mechanism of uptake and trafficking of the individual nanoparticle is dependent on its size, ζ-potential, sequence and density of surface peptides, and other formulation-derived factors. This variability obscures the effect of the surface peptidic residues on the nanoparticle targeting to specific organelles. Nevertheless, we were able to determine that decoration of the nanoparticles with peptidic residues profoundly affected their uptake and intracellular trafficking in the cells, indicating substantial differences in the surface properties between the different formulations. These differences cannot be attributed to the change of the surface charge upon conjugation of the peptidic residues (change of ζ-potential from -32 ± 1 to -27 ± 1 mV). Based on available scientific data on interaction between nanoparticles and immune cells, these small changes in the nanoparticles' ζ-potential are not expected to affect the efficiency of their endocytosis by the dendritic cells,[17] monocytes or macrophages.[26] It is possible that differences in efficiency of endocytosis of the studied formulations derive from specific or nonspecific interactions of surface peptidic residues with the cell membrane that affected the mechanisms of endocytosis. The mechanisms responsible for the lower uptake of unconjugated nanoparticles, as compared to the targeting or control peptide-conjugated nanoparticles, require additional detailed investigation.

Despite the similar extent of endocytosis, control peptide-conjugated nanoparticles preferentially accumulated in the ER, and not the endosomal compartment, while targeting peptide-conjugated nanoparticles have accumulated to a similar extent in these compartments (Figure 4B). The applied pixel-based analysis of the images apparently overestimated the nanoparticle accumulation in the individual organelles[15] due to a limited resolution between the ER (mesh-like network, 50−100 nm diameter of the tubules[27]) and endosomes (tubules with 60−100 nm diameter and up to 4 μm length[28]) and compact morphology/small size of DC2.4 cells. Nevertheless, this analysis can be applied for qualitative or semiquantitative analysis of NP localization in the studied organelles,[15] and the obtained results indicate substantial differences in the intracellular trafficking patterns of the studied nanoparticle formulations.

The preferential colocalization of control peptide-conjugated nanoparticles in the ER was not expected and requires further investigation. It is possible that surface peptidic residues affect the efficiency of individual endocytosis pathways of the nanoparticles and affect their ability to reach the cytosol and the target organelle. The extent of targeting, therefore, can be affected by the relative efficiency of the individual endocytosis mechanisms in the specific cell type.[29] These factors are apparently responsible for the different extent of endocytosis and ER delivery of peptide-conjugated formulations in dendritic cells (this study) vs endothelial cells (HeLa cells[15]). Further studies are required to reveal the mechanisms of uptake and of intracellular trafficking of these formulations by the cells and to determine the potential of decoration of nanoparticles with peptidic residues for intracellularly targeted drug delivery. For this purpose, potent targeting residues should be identified and their targeting properties should be quantitatively assessed (e.g., using imaging and biochemical

approaches[30]) to determine the minimal required amount of targeting moieties, maximal nanoparticle size, and other factors that can limit effectiveness of intracellular drug targeting.[5]

The Effect of Intracellular Targeting of Antigenic Peptides on Their Cross-Presentation. The experimental results (Figure 5) apparently reflect existence of two routes of antigenic peptide cross-presentation under the applied conditions (*in vitro* incubation of DC2.4 cells with the nanoparticles in 24-well plates). The first route involves loading the H-2K^b molecules with soluble SIINFEKL peptide present in the medium.[31,32] The peptide source in this route is the exogenously added SIINFEKL solution, or peptide released into the medium from the nanoparticles that have not been endocytosed (e.g., due to the "burst effect"). Cross-presentation of soluble peptide can take place at the cell surface,[31,33] or at the endosomal (phagosomal or ER-endosomal) compartment,[34] and the magnitude of these processes declines rapidly (see the SIINFEKL solution curve in Figure 5B) reflecting rapid degradation of the soluble peptide in the medium. As compared to *in vitro* experiments, this route is not expected to contribute significantly to prolonged peptide cross-presentation under *in vivo* conditions due to a high dilution and rapid degradation of the unprotected/soluble peptide in the tissue fluids following administration.

The second route involves endocytosis of nanoparticles, prolonged release of the encapsulated antigenic peptide at the organelles that were reached by the nanoparticles, and peptide trafficking and interaction with intracellular H-2K^b molecules. As discussed previously, control peptide-conjugated nanoparticles accumulated to a higher extent in the ER, as compared to the targeting peptide-conjugated nanoparticles (see Figure 4B). We expected that this accumulation in the ER would be accompanied by increased ER delivery and enhanced cross-presentation of antigenic peptide. However, cross-presentation efficiency of control and targeting peptide-conjugated nanoparticles was similar, and was lower as compared to other formulations (see Figure 5). It is possible that this outcome stems from low amount of the antigenic peptide delivered to the intracellular organelles by these formulations (i.e., following substantial release of the antigenic peptide during the conjugation procedure). Therefore, the nanoparticles' preparation and conjugation procedure should be further optimized to increase the loading capacity of the conjugated formulations.

Future studies should also assess the *in vivo* anticancer vaccination efficiency of the developed formulations in animals with established tumors and in tumor protection assays. The developed formulations are expected to be endocytosed by the antigen-presenting cells following vaccination, and that gradual release of the antigenic peptide in the ER and endosomal compartments (the major sites of antigen cross-presentation) will result in prolonged cross-presentation of the antigen by the antigen-presenting cells leading to enhanced activation of cytotoxic T lymphocytes (CTLs) directed against the tumor cells.[35,36] During vaccination experiments, part of the administered formulations will be endocytosed also by the cells of the mononuclear phagocyte system (MPS, formerly known as reticuloendothelial system), primarily by monocytes and macrophages.[37,38] Some macrophages are capable to cross-present endocytosed antigens, and both macrophages and monocytes play a role in tumor immunology and can affect the outcomes of anticancer vaccination experiments. Therefore, planning of vaccination experiments should take into account endocytosis and intracellular trafficking of the studied formulations by the cells of the mononuclear phagocyte system and subsequent pharmacological and immunological consequences of these processes.

Efficient targeting of antigenic peptides to the ER for the purpose of anticancer vaccination was reported previously by Nakagawa et al.[39,40] In these studies a different experimental approach was used: the targeting residues were attached to the drug itself (the antigenic peptide) and not to the carrier (the nanoparticles or liposomes). Poly(γ-glutamic acid) nanoparticles[39] or fusogenic liposomes[40] encapsulating the ER-targeted antigenic peptides induced potent *in vitro* CD8$^+$ T cell activation and enhanced *in vivo* CTL activation and antitumor effects in animal models. The authors suggested that this outcome stems from prolonged cross-presentation of the antigenic peptide due to its efficient targeting to the ER and long-term retention in this organelle (which is characterized by low proteolytic activity as compared to the cytosol).

We chose a different experimental approach and conjugated the targeting residues to the carrier (the nanoparticles) and not to the drug itself (the antigenic peptide). Success of this approach is dependent on capability of the intracellular trafficking mechanisms to handle cargo (nanoparticles) of the size comparable to some intracellular vesicles (hundreds of nanometers in diameter). The drawbacks of this approach include use of a relatively sophisticated 3-step procedure for conjugation of peptide residues that leads to partial release of the encapsulated materials during the conjugation and washing steps. Moreover, quantitative characterization of the peptide-conjugated nanoparticles in terms of conjugation efficiency and stability of surface peptidic residues *in vitro* and *in vivo* is difficult due to analytical limitations. On the other hand, the applied approach is based on the commonly used PLGA nanoparticles and well-studied chemical reactions that are suitable for medical applications and can be easily adapted for different cargo (encapsulation of other drug or multiple drugs) and targeting to different organelle (conjugation of different targeting moieties using the same chemistry).

CONCLUSIONS

Intracellularly targeted drug delivery is a promising new approach for enhancing and controlling the drug pharmacological activities. It appears that conjugation of specific targeting residues can affect the intracellular fate of the nanoparticle drug delivery systems and result in its preferential drug accumulation within specific organelles. Unexpectedly, following endocytosis by DC2.4 cells, nanoparticles decorated with ER-targeting peptide accumulated to a lower extent in the ER as compared to the control peptide-conjugated nanoparticles. We attribute this finding to effect of control and targeting peptides on efficiency of the individual endocytosis pathways of the studied formulations and on their subsequent intracellular distribution. Studies that quantitatively assess the mechanisms, barriers, and efficiency of intracellular drug delivery are required to identify potent targeting residues, to attain efficient intracellular targeting of nanodelivery systems and to determine its therapeutic potential for anticancer vaccination and other applications.

AUTHOR INFORMATION

Corresponding Author

*Department of Pharmacology, Ben-Gurion University of the Negev, POB 653, Beer-Sheva 84105, Israel. Tel: +972-8-6477381. Fax: +972-8-6479303. E-mail: davidst@bgu.ac.il.

Author Contributions

[†]These authors equally contributed to this project.

■ ACKNOWLEDGMENT

This study was supported by the New Faculty Member Grant (Ben-Gurion University of the Negev) and Prof. Yannai Tabb Cancer Research Foundation Grant to D.S. We thank Mrs. Mazal Rubin for technical assistance and Prof. Peter Cresswell (Dept. of Immunobiology, Yale University), Dr. Ayelet David and Prof. Sofia Schreiber-Avissar (Dept. of Pharmacology, Ben-Gurion University), Prof. Lea Eisenbach (Dept. of Immunology, Weizmann Institute of Science), Prof. Smadar Cohen (Dept. of Biotechnology Engineering, Ben-Gurion University), and Prof. Angel Porgador (Dept. of Microbiology and Immunology, Ben-Gurion University) for reagents and research tools.

■ REFERENCES

(1) Burgdorf, S.; Kautz, A.; Bohnert, V.; Knolle, P. A.; Kurts, C. Distinct pathways of antigen uptake and intracellular routing in CD4 and CD8 T cell activation. *Science* **2007**, *316*, 612–6.

(2) Miaczynska, M.; Stenmark, H. Mechanisms and functions of endocytosis. *J. Cell Biol.* **2008**, *180*, 7–11.

(3) Torchilin, V. P. Recent approaches to intracellular delivery of drugs and DNA and organelle targeting. *Annu. Rev. Biomed. Eng.* **2006**, *8*, 343–75.

(4) Breunig, M.; Bauer, S.; Goepferich, A. Polymers and nanoparticles: intelligent tools for intracellular targeting?. *Eur. J. Pharm. Biopharm.* **2008**, *68*, 112–28.

(5) Stepensky, D. Quantitative aspects of intracellularly-targeted drug delivery. *Pharm. Res.* **2010**, *27*, 2776–80.

(6) Reichert, J. M.; Wenger, J. B. Development trends for new cancer therapeutics and vaccines. *Drug Discovery Today* **2008**, *13*, 30–7.

(7) Purcell, A. W.; McCluskey, J.; Rossjohn, J. More than one reason to rethink the use of peptides in vaccine design. *Nat. Rev. Drug Discovery* **2007**, *6*, 404–14.

(8) Amigorena, S.; Savina, A. Intracellular mechanisms of antigen cross presentation in dendritic cells. *Curr. Opin. Immunol.* **2010**, *22*, 109–17.

(9) Teasdale, R. D.; Jackson, M. R. Signal-mediated sorting of membrane proteins between the endoplasmic reticulum and the Golgi apparatus. *Annu. Rev. Cell Dev. Biol.* **1996**, *12*, 27–54.

(10) Andersson, H.; Kappeler, F.; Hauri, H. P. Protein targeting to endoplasmic reticulum by dilysine signals involves direct retention in addition to retrieval. *J. Biol. Chem.* **1999**, *274*, 15080–4.

(11) Sanderson, S.; Shastri, N. LacZ inducible, antigen/MHC-specific T cell hybrids. *Int. Immunol.* **1994**, *6*, 369–76.

(12) Jiang, X.; Zhang, J.; Zhou, Y.; Xu, J.; Liu, S. Facile preparation of core-crosslinked micelles from azide-containing thermoresponsive double hydrophilic diblock copolymer via Click chemistry. *J. Polym. Sci., Part A: Polym. Chem.* **2008**, *46*, 860–71.

(13) Rasband, W. S. *ImageJ*; U. S. National Institutes of Health: Bethesda, Maryland, USA, http://rsb.info.nih.gov/ij/, 1997−2010.

(14) Stepensky, D. "IntraCell"—intracellular localization of nanoparticles in the individual organelles, plugin for ImageJ. Online. 2011. Available from http://rsb.info.nih.gov/ij/plugins/intracell/.

(15) Sneh-Edri, H.; Stepensky, D. "IntraCell" plugin for assessment of intracellular localization of nano-delivery systems and their targeting to the individual organelles. *Biochem. Biophys. Res. Commun.* **2011**, *405*, 228–33.

(16) Waeckerle-Men, Y.; Groettrup, M. PLGA microspheres for improved antigen delivery to dendritic cells as cellular vaccines. *Adv. Drug Delivery Rev.* **2005**, *57*, 475–82.

(17) Foged, C.; Brodin, B.; Frokjaer, S.; Sundblad, A. Particle size and surface charge affect particle uptake by human dendritic cells in an in vitro model. *Int. J. Pharm.* **2005**, *298*, 315–22.

(18) Bachmann, M. F.; Jennings, G. T. Vaccine delivery: a matter of size, geometry, kinetics and molecular patterns. *Nat. Rev. Immunol.* **2010**, *10*, 787–96.

(19) Hoshino, A.; Fujioka, K.; Oku, T.; Nakamura, S.; Suga, M.; Yamaguchi, Y.; Suzuki, K.; Yasuhara, M.; Yamamoto, K. Quantum dots targeted to the assigned organelle in living cells. *Microbiol. Immunol.* **2004**, *48*, 985–94.

(20) Misra, R.; Sahoo, S. K. Intracellular trafficking of nuclear localization signal conjugated nanoparticles for cancer therapy. *Eur. J. Pharm. Sci.* **2010**, *39*, 152–63.

(21) Panyam, J.; Zhou, W. Z.; Prabha, S.; Sahoo, S. K.; Labhasetwar, V. Rapid endo-lysosomal escape of poly(DL-lactide-co-glycolide) nanoparticles: implications for drug and gene delivery. *FASEB J.* **2002**, *16*, 1217–26.

(22) Keegan, M. E.; Royce, S. M.; Fahmy, T.; Saltzman, W. M. In vitro evaluation of biodegradable microspheres with surface-bound ligands. *J. Controlled Release* **2006**, *110*, 574–80.

(23) Wang, Q.; Wang, J.; Lu, Q.; Detamore, M. S.; Berkland, C. Injectable PLGA based colloidal gels for zero-order dexamethasone release in cranial defects. *Biomaterials* **2010**, *31*, 4980–6.

(24) Lo, C. T.; Van Tassel, P. R.; Saltzman, W. M. Simultaneous release of multiple molecules from poly(lactide-co-glycolide) nanoparticles assembled onto medical devices. *Biomaterials* **2009**, *30*, 4889–97.

(25) Zhang, N.; Chittasupho, C.; Duangrat, C.; Siahaan, T. J.; Berkland, C. PLGA nanoparticle−peptide conjugate effectively targets intercellular cell-adhesion molecule-1. *Bioconjugate Chem.* **2008**, *19*, 145–52.

(26) Verma, A.; Stellacci, F. Effect of surface properties on nanoparticle-cell interactions. *Small* **2011**, *6*, 12–21.

(27) Voeltz, G. K.; Prinz, W. A. Sheets, ribbons and tubules - how organelles get their shape. *Nat. Rev. Mol. Cell Biol.* **2007**, *8*, 258–64.

(28) Marsh, M.; Griffiths, G.; Dean, G. E.; Mellman, I.; Helenius, A. Three-dimensional structure of endosomes in BHK-21 cells. *Proc. Natl. Acad. Sci. U.S.A.* **1986**, *83*, 2899–903.

(29) Cartiera, M. S.; Johnson, K. M.; Rajendran, V.; Caplan, M. J.; Saltzman, W. M. The uptake and intracellular fate of PLGA nanoparticles in epithelial cells. *Biomaterials* **2009**, *30*, 2790–8.

(30) Cardarelli, F.; Serresi, M.; Albanese, A.; Bizzarri, R.; Beltram, F. Quantitative analysis of Tat peptide binding to import carriers reveals unconventional nuclear transport properties. *J. Biol. Chem.* **2011**, *286*, 12292–9.

(31) Met, O.; Buus, S.; Claesson, M. H. Peptide-loaded dendritic cells prime and activate MHC-class I-restricted T cells more efficiently than protein-loaded cross-presenting DC. *Cell. Immunol.* **2003**, *222*, 126–33.

(32) Porgador, A.; Gilboa, E. Bone marrow-generated dendritic cells pulsed with a class I-restricted peptide are potent inducers of cytotoxic T lymphocytes. *J. Exp. Med.* **1995**, *182*, 255–60.

(33) Smyth, L. A.; Harker, N.; Turnbull, W.; El-Doueik, H.; Klavinskis, L.; Kioussis, D.; Lombardi, G.; Lechler, R. The relative efficiency of acquisition of MHC:peptide complexes and cross-presentation depends on dendritic cell type. *J. Immunol.* **2008**, *181*, 3212–20.

(34) Ackerman, A. L.; Cresswell, P. Cellular mechanisms governing cross-presentation of exogenous antigens. *Nat. Immunol.* **2004**, *5*, 678–84.

(35) Audran, R.; Peter, K.; Dannull, J.; Men, Y.; Scandella, E.; Groettrup, M.; Gander, B.; Corradin, G. Encapsulation of peptides in biodegradable microspheres prolongs their MHC class-I presentation by dendritic cells and macrophages in vitro. *Vaccine* **2003**, *21*, 1250–5.

(36) Waeckerle-Men, Y.; Allmen, E. U.; Gander, B.; Scandella, E.; Schlosser, E.; Schmidtke, G.; Merkle, H. P.; Groettrup, M. Encapsulation of proteins and peptides into biodegradable poly(D,L-lactide-co-glycolide) microspheres prolongs and enhances antigen presentation by human dendritic cells. *Vaccine* **2006**, *24*, 1847–57.

(37) Panagi, Z.; Beletsi, A.; Evangelatos, G.; Livaniou, E.; Ithakissios, D. S.; Avgoustakis, K. Effect of dose on the biodistribution and pharmacokinetics of PLGA and PLGA-mPEG nanoparticles. *Int. J. Pharm.* **2001**, *221*, 143–52.

(38) Semete, B.; Booysen, L.; Lemmer, Y.; Kalombo, L.; Katata, L.; Verschoor, J.; Swai, H. S. In vivo evaluation of the biodistribution and

safety of PLGA nanoparticles as drug delivery systems. *Nanomedicine* **2010**, *6*, 662–71.

(39) Matsuo, K.; Yoshikawa, T.; Oda, A.; Akagi, T.; Akashi, M.; Mukai, Y.; Yoshioka, Y.; Okada, N.; Nakagawa, S. Efficient generation of antigen-specific cellular immunity by vaccination with poly(gamma-glutamic acid) nanoparticles entrapping endoplasmic reticulum-targeted peptides. *Biochem. Biophys. Res. Commun.* **2007**, *362*, 1069–72.

(40) Hayashi, A.; Wakita, H.; Yoshikawa, T.; Nakanishi, T.; Tsutsumi, Y.; Mayumi, T.; Mukai, Y.; Yoshioka, Y.; Okada, N.; Nakagawa, S. A strategy for efficient cross-presentation of CTL-epitope peptides leading to enhanced induction of in vivo tumor immunity. *J. Controlled Release* **2007**, *117*, 11–9.